

Four-body effects on ${}^9\text{Be}+{}^{208}\text{Pb}$ scattering and fusion around the Coulomb barrier

P Descouvemont¹, T Druet¹, L F Canto^{2,3} and M S Hussein^{4,5,6}

¹ Physique Nucléaire Théorique et Physique Mathématique, C.P. 229, Université Libre de Bruxelles (ULB), B 1050 Brussels, Belgium

² Instituto de Física, Universidade Federal do Rio de Janeiro, C.P. 68528, 21941-972 Rio de Janeiro, RJ, Brazil

³ Instituto de Física, Universidade Federal Fluminense, Av. Gal. Milton Tavares de Souza s/n, Niterói, RJ, Brazil

⁴ Departamento de Física Matemática, Instituto de Física, Universidade de São Paulo, C.P. 66318, 05314-970, São Paulo, SP, Brazil

⁵ Instituto de Estudos Avançados, Universidade de São Paulo, C.P. 72012, 05508-970, São Paulo, SP, Brazil

⁶ Departamento de Física, Instituto Tecnológico de Aeronáutica, CTA, São José dos Campos, São Paulo, SP, Brazil

E-mail: pdesc@ulb.ac.be

Abstract. We investigate the ${}^9\text{Be}+{}^{208}\text{Pb}$ elastic scattering and fusion at energies around the Coulomb barrier. The ${}^9\text{Be}$ nucleus is described in a $\alpha + \alpha + n$ three-body model, using the hyperspherical coordinate method. The scattering with ${}^{208}\text{Pb}$ is then studied with the Continuum Discretized Coupled Channel (CDCC) method, where the $\alpha + \alpha + n$ continuum is approximated by a discrete number of pseudostates. Optical potentials for the $\alpha+{}^{208}\text{Pb}$ and $n+{}^{208}\text{Pb}$ systems are taken from the literature. We present elastic-scattering and fusion cross sections at different energies, and investigate the convergence with respect to the truncation of the $\alpha + \alpha + n$ continuum. A good agreement with experiment is obtained, considering that there is no parameter fitting. We show that continuum effects increase at low energies.

1. Introduction

Many experiments have been performed with the ${}^9\text{Be}$ nucleus, used as a target or as a projectile [1]. Although ${}^9\text{Be}$ is stable, it presents a Borromean structure, as the well known halo nucleus ${}^6\text{He}$. None of the two-body subsystems $\alpha + n$ or $\alpha + \alpha$ is bound in ${}^9\text{Be}$, which has important consequences on the theoretical description of this nucleus. Precise wave functions must include the three-body nature of ${}^9\text{Be}$. The hyperspherical formalism [2] is an ideal tool to describe three-body Borromean systems, as it does not assume a specific two-body structure, and considers the three particles $\alpha + \alpha + n$ on an equal footing.

In the present work, we aim at investigating ${}^9\text{Be}$ scattering and fusion on an heavy target. The reaction framework is the Continuum Discretized Coupled Channel (CDCC) method [3–5], which is well adapted to weakly bound projectiles since it allows to include breakup channels. Over the last decades, the CDCC method has been extended in various directions, and in particular to reactions involving three-body projectiles such as ${}^6\text{He}$ [6] or ${}^{11}\text{Li}$ [7]. Going from two-body projectiles (such as $d=p+n$ or ${}^7\text{Li}=\alpha+t$) to three-body projectiles strongly increases

the complexity of the calculations, even if both options eventually end up with a standard coupled-channel system.

Many data have been obtained for ${}^9\text{Be}+{}^{208}\text{Pb}$ elastic scattering [8, 9] and fusion [10, 11]. These experimental data provide a good opportunity to test ${}^9\text{Be}$ wave functions. Previous CDCC calculations, using a two-body approximation for ${}^9\text{Be}$, show that breakup effects are important [9, 12, 13]. In a two-body model, ${}^9\text{Be}$ is assumed to have a ${}^8\text{Be} + n$ or ${}^5\text{He} + \alpha$ cluster structure. This approximation presents several shortcomings: (i) ${}^8\text{Be}$ and ${}^5\text{He}$ are unbound, and assuming a point-like structure is questionable; (ii) in a more rigorous three-body approach, both configurations are strictly equivalent, and the relative importance of the ${}^8\text{Be} + n$ and ${}^5\text{He} + \alpha$ channels is not relevant; (iii) a two-body model of ${}^9\text{Be}$ requires ${}^8\text{Be}+{}^{208}\text{Pb}$ and ${}^5\text{He}+{}^{208}\text{Pb}$ optical potentials, which are not available. These different issues are more precisely addressed in a three-body model of ${}^9\text{Be}$. No assumption should be made about the cluster structure, and $\alpha+{}^{208}\text{Pb}$ as well as $n+{}^{208}\text{Pb}$ optical potentials are available in the literature.

2. Three-body model of ${}^9\text{Be}$

The determination of the ${}^9\text{Be}$ wave functions is the first step for the ${}^9\text{Be}+{}^{208}\text{Pb}$ CDCC calculation. The spectroscopy of ${}^9\text{Be}$ in cluster models has been performed in previous microscopic [14–16] and non-microscopic [17–19] models. For a three-body system, the Hamiltonian is given by

$$H_0 = \sum_{i=1}^3 \frac{\mathbf{p}_i^2}{2m_i} + \sum_{i<j=1}^3 V_{ij}(\mathbf{r}_i - \mathbf{r}_j), \quad (1)$$

where \mathbf{r}_i and \mathbf{p}_i are the space and momentum coordinates of the three particles with masses m_i , and V_{ij} a potential between nuclei i and j . For the $\alpha + \alpha$ interaction, we use the deep potential of Buck *et al.* [20]. The $\alpha+n$ interaction is taken from Kanada *et al.* [21]. Both (real) potentials accurately reproduce the $\alpha + \alpha$ and α +nucleon phase shifts over a wide energy range.

With these potentials, the ${}^9\text{Be}$ ground state is too bound (-3.12 MeV, while the experimental value is -1.57 MeV with respect to the $\alpha + \alpha + n$ threshold). We have therefore introduced a phenomenological three-body force as

$$V_{3B}(\rho) = \frac{V_0}{1 + (\rho/\rho_0)^2}, \quad (2)$$

where $\rho_0 = 6$ fm [22]. Using $V_0 = 2.7$ MeV provides the experimental binding energy of the $3/2^-$ ground state. The r.m.s. radius, the quadrupole moment, and the magnetic moment are $\sqrt{r^2} = 2.36$ fm, $Q(3/2^-) = 4.96$ e.fm², and $\mu = -1.33$ μ_N , respectively. These values are in fair agreement with experiment (2.45 ± 0.01 fm, 5.29 ± 0.04 e.fm² and -1.18 μ_N , respectively)

3. The CDCC method

We present here a brief outline of the CDCC method, and we refer to Ref. [23] for specificities of three-body projectiles. The CDCC method is based on approximate solutions of the projectile Hamiltonian (1)

$$H_0 \Phi_k^{jm\pi} = E_{0,k}^{j\pi} \Phi_k^{jm\pi}, \quad (3)$$

where k are the excitation levels in partial wave $j\pi$. Solutions with $E_{0,k}^{j\pi} < 0$ correspond to bound states of the projectile, whereas $E_{0,k}^{j\pi} > 0$ correspond to narrow resonances or to approximations of the three-body continuum. These states cannot be associated with physical states, and are referred to as pseudostates.

The Hamiltonian of the projectile + target system is written as

$$H(\mathbf{R}, \mathbf{x}, \mathbf{y}) = H_0(\mathbf{x}, \mathbf{y}) - \frac{\hbar^2}{2\mu_{PT}} \Delta_R + V(\mathbf{R}, \mathbf{x}, \mathbf{y}) \quad (4)$$

where μ_{PT} is the reduced mass of the system, and \mathbf{R} the relative coordinate (see Fig. 1). The Jacobi coordinates \mathbf{x} and \mathbf{y} are proportional to $\mathbf{r}_{\text{Be-n}}$ and $\mathbf{r}_{\alpha-\alpha}$, respectively. The potential term reads

$$V(\mathbf{R}, \mathbf{x}, \mathbf{y}) = V_{1t}(\mathbf{R}, \mathbf{y}) + V_{2t}(\mathbf{R}, \mathbf{x}, \mathbf{y}) + V_{3t}(\mathbf{R}, \mathbf{x}, \mathbf{y}) \quad (5)$$

where the three components V_{it} are optical potentials between fragment i and the target.

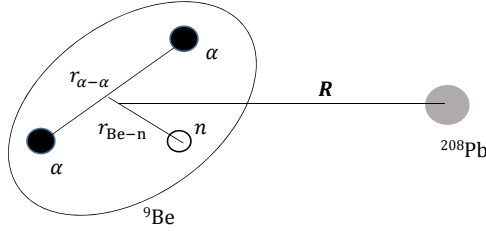


Figure 1. Coordinates involved in the present four-body model.

In order to solve the Schrödinger equation associated with (4), the total wave function with angular momentum J and parity Π is expanded as

$$\Psi_{(\omega)}^{JM\Pi}(\mathbf{R}, \mathbf{x}, \mathbf{y}) = \sum_{j\pi kL} \varphi_{j\pi kL}^{JM\Pi}(\Omega_R, \mathbf{x}, \mathbf{y}) g_{jkL(\omega)}^{J\Pi}(R), \quad (6)$$

where ω is the entrance channel, and where the channel wave functions are given by

$$\varphi_{j\pi kL}^{JM\Pi}(\Omega_R, \mathbf{x}, \mathbf{y}) = i^L \left[\Phi_k^{j\pi}(\mathbf{x}, \mathbf{y}) \otimes Y_L(\Omega_R) \right]^{JM}. \quad (7)$$

The radial functions $g_c^{J\Pi}(R)$ (we use the notation $c = (j, \pi, k, L)$) are obtained from the system

$$\left[-\frac{\hbar^2}{2\mu_{PT}} \left(\frac{d^2}{dR^2} - \frac{L(L+1)}{R^2} \right) + E_c - E \right] g_c^{J\Pi}(R) + \sum_{c'} V_{c,c'}^{J\Pi}(R) g_{c'}^{J\Pi}(R) = 0, \quad (8)$$

where E is the c.m. energy, and where the coupling potentials are given by matrix elements

$$V_{c,c'}^{J\Pi}(R) = \langle \varphi_c^{JM\Pi} | V | \varphi_{c'}^{JM\Pi} \rangle. \quad (9)$$

As the fragment-target potentials (5) are optical potentials, matrix elements (9) contain a real and an imaginary parts. The integration is performed over Ω_R and over the internal coordinates \mathbf{x} and \mathbf{y} . The calculation of these coupling potentials is much more complicated for three-body projectiles than for two-body projectiles. Out of the three potentials V_{it} in (5), matrix elements of V_{1t} are the easiest since V_{1t} does not depend on \mathbf{x} . The calculations of the two remaining terms V_{2t} and V_{3t} are performed by using the Raynal-Revai coefficients (see Refs. [23, 24] for detail). We solve Eq. (8) with the R -matrix theory [25].

4. Application to the ${}^9\text{Be}+{}^{208}\text{Pb}$ system

4.1. Elastic scattering

The calculations are performed with the $j^\pi = 3/2^-, 5/2^-, 1/2^+$ partial waves on ${}^9\text{Be}$, and the cutoff energy is 10 MeV. Figure 2 shows ${}^9\text{Be}+{}^{208}\text{Pb}$ elastic cross sections at various energies (the data are taken from Refs. [8, 26]). In contrast with optical-model calculations [8], no renormalization of the potential is needed. The absorption is simulated by the imaginary parts of the $\alpha-{}^{208}\text{Pb}$ and $n-{}^{208}\text{Pb}$ interactions, and by the $\alpha + \alpha + n$ discretized continuum. From Fig. 2, it appears that continuum couplings are more important at low energies. At $E = 38$ and 44 MeV, the single-channel calculation, limited to the ${}^9\text{Be}$ ground state (dotted lines) is significantly different from the data. This confirms the conclusion of a previous work [27] which suggests that continuum couplings are more important at low energies.

Calculations involving $3/2^-$ pseudostates are shown as dashed lines, and the full calculations as solid lines. The effect of the $1/2^+$ partial wave is minor, and the main differences stem from the $5/2^-$ pseudostates.

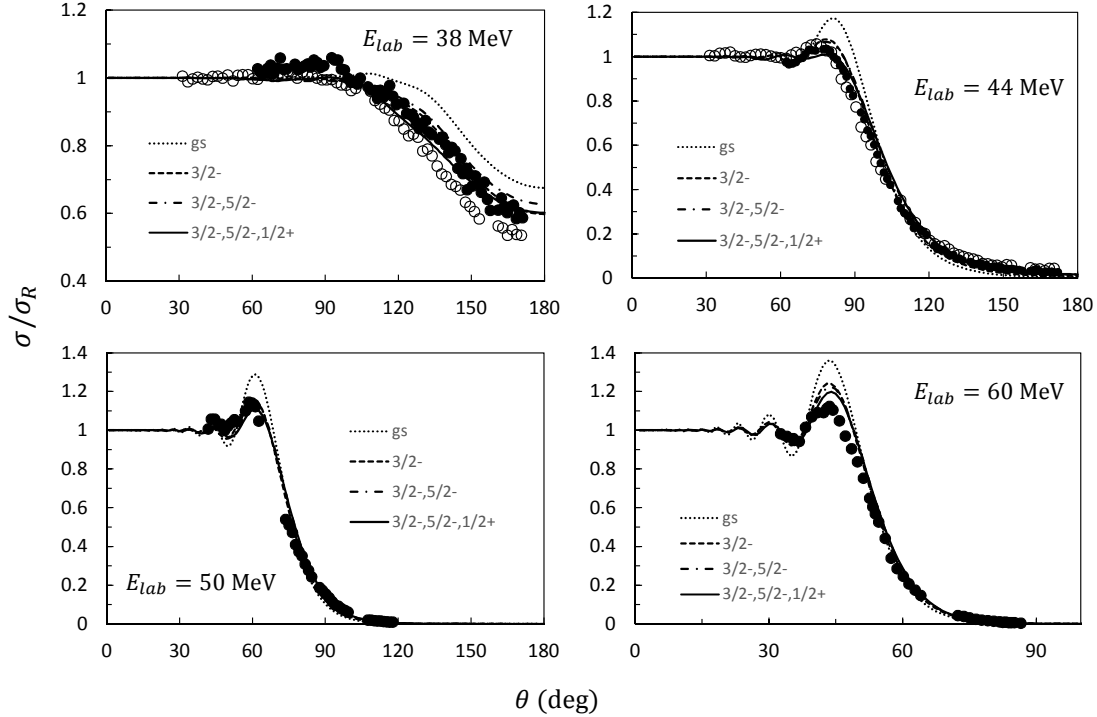


Figure 2. ${}^9\text{Be}+{}^{208}\text{Pb}$ elastic cross sections (divided by the Rutherford cross section) at different ${}^9\text{Be}$ laboratory energies, and for different sets of ${}^9\text{Be}$ partial waves. The experimental data are taken from Ref. [8] (filled circles) and Ref. [26] (open circles).

4.2. Fusion

The ${}^9\text{Be}+{}^{208}\text{Pb}$ fusion reaction has been studied theoretically by several groups (see Ref. [28] and references therein). Data about the various mechanisms (total TF, complete CF and incomplete ICF fusion) are also available in the literature [10, 11, 29].

The total fusion cross section σ_{TF} is defined from [30–32]

$$\sigma_{TF}(E) = \frac{\pi}{k^2} \sum_{J\Pi} (2J+1) T^{J\Pi}(E), \quad (10)$$

where k is the wave number, and $T^{J\Pi}$ is a transmission coefficient in partial wave $J\Pi$. It can be obtained from the scattering matrices as

$$T^{J\Pi}(E) = \frac{1}{(2I_1 + 1)(2I_2 + 1)} \sum_{L\omega, L} (\delta_{L\omega L} - |U_{\omega L\omega, \omega L}^{J\Pi}(E)|^2), \quad (11)$$

where I_1 and I_2 are the spins of the colliding nuclei. Using flux conservation properties, the transmission coefficient can be expressed from the imaginary part $W_{c,c'}^{J\Pi}(R)$ of the coupling potentials [32]. It is therefore strictly equivalent to

$$T^{J\Pi}(E) = -\frac{4k}{E} \frac{1}{(2I_1 + 1)(2I_2 + 1)} \sum_{L\omega} \sum_{\alpha, \alpha', L, L'} \int g_{\omega L\omega, \alpha L}^{J\Pi}(R) W_{\alpha L, \alpha' L'}^{J\Pi}(R) g_{\omega L\omega, \alpha' L'}^{J\Pi}(R) dR, \quad (12)$$

where index α stands for $\alpha = (j, \pi, k)$, i.e. it does not depend on the angular momentum L (in other words $c = (\alpha, L)$). This derivation is more complicated since it requires the wave functions, but it provides a better accuracy at low energies, where the scattering matrix is close to unity. It also provides an approximate method to distinguish between CF and ICF [33].

The TF cross section is shown in logarithmic (Fig. 3) and linear (Fig. 4) scales. Convergence against ${}^9\text{Be}$ states is rather fast, except below the Coulomb barrier where neglecting breakup channels leads to an underestimation of the cross section. Breakup effects, however, introduce a strong enhancement of the cross section at low energies. Similar conclusions have been drawn by Jha *et al.* [28].

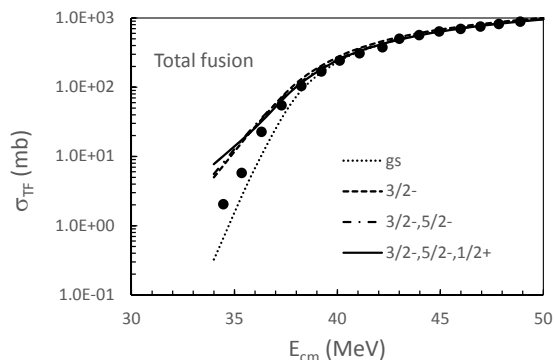


Figure 3. ${}^9\text{Be}+{}^{208}\text{Pb}$ total fusion cross section in a logarithmic scale. The data are taken from [10].

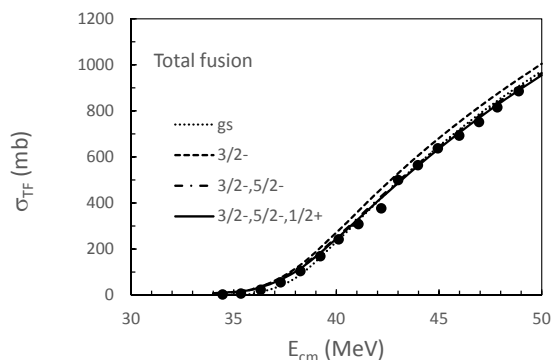


Figure 4. See Fig. 3 in a linear scale.

5. Conclusion

We have applied the CDCC formalism to the ${}^9\text{Be}+{}^{208}\text{Pb}$ system. In a first step, we have computed ${}^9\text{Be}$ wave functions in a three-body $\alpha + \alpha + n$ model. These calculations were performed for low-lying states, but also for pseudostates, which represent positive-energy approximations of the continuum. The main advantage of the hyperspherical approach is that it treats the three-body continuum without any approximation concerning possible ${}^8\text{Be} + n$ or ${}^5\text{He} + \alpha$ cluster structures, which are in fact strictly equivalent.

The three-body model of ${}^9\text{Be}$ relies on $\alpha + \alpha$ and $\alpha + n$ (real) interactions, which reproduce very well the elastic phase shifts. With these bare interactions, the ${}^9\text{Be}$ ground state is slightly too bound. We therefore introduce a phenomenological three-body force to reproduce the

experimental ground-state energy. The spectroscopic properties of low-lying states is in fair agreement with experiment.

We used first the ${}^9\text{Be}$ wave functions in a CDCC calculation of the ${}^9\text{Be}+{}^{208}\text{Pb}$ elastic scattering at energies close to the Coulomb barrier. As expected, including continuum channels improves the theoretical cross sections. A fair agreement with the data is obtained.

We also applied the four-body CDCC to the ${}^9\text{Be}+{}^{208}\text{Pb}$ fusion, by using the same potentials as for elastic scattering. The total fusion cross section is found in good agreement with experiment, except at very low energies, where we overestimate the data.

References

- [1] Keeley N, Alamanos N, Kemper K and Rusek K 2009 *Prog. Part. Nucl. Phys.* **63** 396
- [2] Zhukov M V, Danilin B V, Fedorov D V, Bang J M, Thompson I J and Vaagen J S 1993 *Phys. Rep.* **231** 151
- [3] Rawitscher G H 1974 *Phys. Rev. C* **9** 2210
- [4] Yahiro M, Iseri Y, Kameyama H, Kamimura M and Kawai M 1986 *Prog. Theor. Phys. Suppl.* **89** 32
- [5] Yahiro M, Matsumoto T, Minomo K, Sumi T and Watanabe S 2012 *Prog. Theor. Phys. Suppl.* **196** 87
- [6] Matsumoto T, Hiyama E, Ogata K, Iseri Y, Kamimura M, Chiba S and Yahiro M 2004 *Phys. Rev. C* **70** 061601
- [7] Cubero M, Fernández-García J P, Rodríguez-Gallardo M, Acosta L, Alcorta M, Alvarez M A G, Borge M J G, Buchmann L, Diget C A, Falou H A, Fulton B R, Fynbo H O U, Galaviz D, Gómez-Camacho J, Kanungo R, Lay J A, Madurga M, Martel I, Moro A M, Mukha I, Nilsson T, Sánchez-Benítez A M, Shotter A, Tengblad O and Walden P 2012 *Phys. Rev. Lett.* **109** 262701
- [8] Woolliscroft R J, Fulton B R, Cowin R L, Dasgupta M, Hinde D J, Morton C R and Berriman A C 2004 *Phys. Rev. C* **69** 044612
- [9] Pandit S K, Jha V, Mahata K, Santra S, Palshetkar C S, Ramachandran K, Parkar V V, Shrivastava A, Kumawat H, Roy B J, Chatterjee A and Kailas S 2011 *Phys. Rev. C* **84** 031601
- [10] Dasgupta M, Hinde D J, Butt R D, Anjos R M, Berriman A C, Carlin N, Gomes P R S, Morton C R, Newton J O, Szanto de Toledo A and Hagino K 1999 *Phys. Rev. Lett.* **82** 1395
- [11] Dasgupta M, Gomes P R S, Hinde D J, Moraes S B, Anjos R M, Berriman A C, Butt R D, Carlin N, Lubian J, Morton C R, Newton J O and Szanto de Toledo A 2004 *Phys. Rev. C* **70** 024606
- [12] Keeley N, Kemper K W and Rusek K 2001 *Phys. Rev. C* **64** 031602
- [13] Parkar V V, Jha V, Pandit S K, Santra S and Kailas S 2013 *Phys. Rev. C* **87** 034602
- [14] Descouvemont P 2001 *Eur. Phys. J. A* **12** 413
- [15] Arai K, Descouvemont P, Baye D and Catford W N 2003 *Phys. Rev. C* **68** 014310
- [16] Arai K, Ogawa Y, Suzuki Y and Varga K 1996 *Phys. Rev. C* **54** 132
- [17] Voronchev V, Kukulín V, Pomerantsev V and Ryzhikh G 1995 *Few-Body Systems* **18** 191
- [18] Theeten M, Baye D and Descouvemont P 2006 *Phys. Rev. C* **74** 044304
- [19] Álvarez-Rodríguez R, Jensen A S, Garrido E and Fedorov D V 2010 *Phys. Rev. C* **82** 034001
- [20] Buck B, Friedrich H and Wheatley C 1977 *Nucl. Phys. A* **275** 246
- [21] Kanada H, Kaneko T, Nagata S and Nomoto M 1979 *Prog. Theor. Phys.* **61** 1327
- [22] Thompson I J, Danilin B V, Efros V D, Vaagen J S, Bang J M and Zhukov M V 2000 *Phys. Rev. C* **61** 024318
- [23] Rodríguez-Gallardo M, Arias J M, Gómez-Camacho J, Johnson R C, Moro A M, Thompson I J and Tostevin J A 2008 *Phys. Rev. C* **77** 064609
- [24] Thompson I J, Nunes F M and Danilin B V 2004 *Comp. Phys. Comm.* **161** 87
- [25] Descouvemont P and Baye D 2010 *Rep. Prog. Phys.* **73** 036301
- [26] Yu N, Zhang H Q, Jia H M, Zhang S T, Ruan M, Yang F, Wu Z D, Xu X X and Bai C L 2010 *J. Phys. G* **37** 075108
- [27] Druet T and Descouvemont P 2012 *Eur. Phys. J. A* **48** 147
- [28] Jha V, Parkar V V and Kailas S 2014 *Phys. Rev. C* **89** 034605
- [29] Dasgupta M, Hinde D J, Sheehy S L and Bouriquet B 2010 *Phys. Rev. C* **81** 024608
- [30] Canto L F, Gomes P R S, Donangelo R and Hussein M S 2006 *Phys. Rep.* **424** 1
- [31] Hagino K and Takigawa N 2012 *Prog. Theor. Phys.* **128** 1001–1060
- [32] Canto L F and Hussein M S 2013 *Scattering Theory of Molecules, Atoms and Nuclei* (World Scientific Publishing)
- [33] Diaz-Torres A and Thompson I J 2002 *Phys. Rev. C* **65** 024606